Understanding and improving the reusability of phosphate adsorbents for wastewater effluent polishing

Suresh Kumar, Prashanth; Ejerssa, Wondesen Workneh; Wegener, Carita Clarissa; Korving, Leon; Dugulan, Achim Iulian; Temmink, Hardy; van Loosdrecht, Mark C.M.; Witkamp, Geert Jan

DOI
10.1016/j.watres.2018.08.040

Publication date
2018

Document Version
Accepted author manuscript

Published in
Water Research

Citation (APA)
Suresh Kumar, P., Ejerssa, W. W., Wegener, C. C., Korving, L., Dugulan, A. I., Temmink, H., van Loosdrecht, M. C. M., & Witkamp, G. J. (2018). Understanding and improving the reusability of phosphate adsorbents for wastewater effluent polishing. *Water Research*, *145*, 365-374. https://doi.org/10.1016/j.watres.2018.08.040

Understanding and improving the reusability of phosphate adsorbents for wastewater effluent polishing

Prashanth Suresh Kumar[a,b*], *Wondesen Workneh Ejerssa*[a], *Carita Clarissa Wegener*[c], *Leon Korving*[a*], *Achim Iulian Dugulan*[d], *Hardy Temmink*[a,e], *Mark C.M. van Loosdrecht*[b], *Geert-Jan Witkamp*[b,1]

[a]Wetsus, European Centre Of Excellence for Sustainable Water Technology, Oostergoweg 9, 8911 MA, Leeuwarden, The Netherlands

[b]Department of Biotechnology, Applied Sciences, Delft University of Technology, Building 58, Van der Maasweg 9, 2629 HZ Delft, The Netherlands

[c]Chair for Mechanical Process Engineering / Water Technology, Faculty of Engineering, University Duisburg-Essen, Lotharstrasse 1, 47057 Duisburg, Germany

[d]Fundamental Aspects of Materials and Energy Group, Delft University of Technology, Mekelweg 15, 2629 JB Delft, The Netherlands

[e]Sub-department of Environmental technology, Wageningen University and Research, Bornse Weilanden 9, 6708 WG, Wageningen, The Netherlands.

[1]Current address: King Abdullah University of Science and Technology (KAUST), Water Desalination and Reuse Center (WDRC), Division of Biological and Environmental Science and Engineering (BESE), Thuwal, 23955-6900, Saudi Arabia.

*Corresponding author: psureshkumar@tudelft.nl; Department of Biotechnology, Applied Sciences, Delft University of Technology, Building 58, Van der Maasweg 9, 2629 HZ Delft, The Netherlands

Graphical abstract

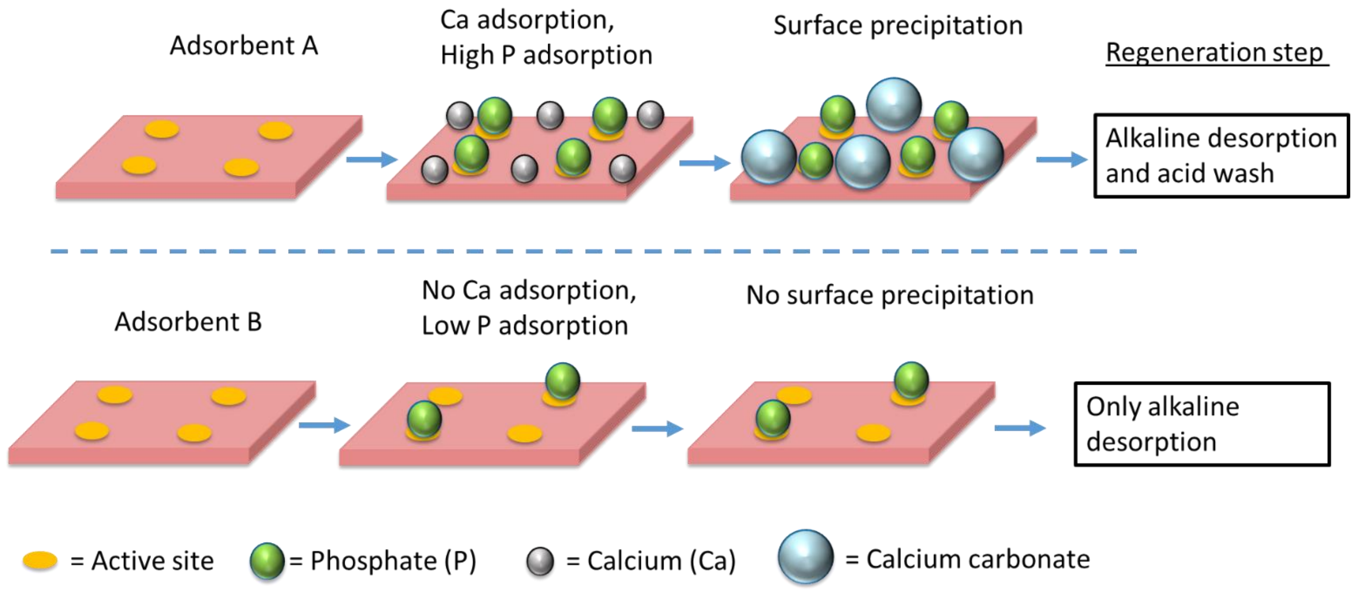

Abstract

Phosphate is a vital nutrient for life but its discharge from wastewater effluents can lead to eutrophication. Adsorption can be used as effluent polishing step to reduce phosphate to very low concentrations. Adsorbent reusability is an important parameter to make the adsorption process economically feasible. This implies that the adsorbent can be regenerated and used over several cycles without appreciable performance decline. In the current study, we have studied the phosphate adsorption and reusability of commercial iron oxide based adsorbents for wastewater effluent. Effects of adsorbent properties like particle size, surface area, type of iron oxide, and effects of some competing ions were determined. Moreover the effects of regeneration methods, which include an alkaline desorption step and an acid wash step, were studied. It was found that reducing the adsorbent particle size increased the phosphate adsorption of porous adsorbents significantly. Amongst all the other parameters, calcium had the greatest influence on phosphate adsorption and adsorbent reusability. Phosphate adsorption was enhanced by co-adsorption of calcium, but calcium formed surface precipitates such as calcium carbonate. These surface precipitates affected the adsorbent reusability and needed to be removed by implementing an acid wash step. The insights from this study are useful in designing optimal regeneration procedures and improving the lifetime of phosphate adsorbents used for wastewater effluent polishing.

Key words: Phosphate adsorption, wastewater effluent, regeneration, reusability, surface precipitation, calcium adsorption

1. Introduction

Phosphate, the common form of inorganic phosphorous, is a vital nutrient for life and an essential component of food. Humans consume phosphate as food which subsequently ends up in municipal wastewater plants (Cordell et al. 2009). Discharge of phosphate from the wastewater effluent even in the range of micrograms per liter can cause eutrophication of surface water (L. Correll 1998). Adsorption is often suggested as a polishing step but for the process to be economically feasible, either the adsorbent needs to be extremely cheap or be reusable (Li et al. 2016, Loganathan et al. 2014). Effective reusability means the adsorbent can be regenerated and used again for several cycles without diminishing its adsorption capacity. The reusability of the adsorbent via regeneration also enables phosphate recovery and contributes to a circular economy.

Many studies focus on producing phosphate adsorbents with high adsorption capacity but fewer studies touch on the reusability aspect (Li et al. 2016). An adsorbent's performance can decrease over time due to multiple reasons. These include incomplete desorption of adsorbate, surface precipitation, loss of active sites due to adsorbent wear and tear, and changes in adsorbent properties like surface area, porosity, crystallinity during adsorption and regeneration (Cabrera et al. 1981, Chitrakar et al. 2006, Kunaschk et al. 2015). The reusability of the adsorbents becomes an issue especially in a complex matrix like wastewater effluent where several ions can bind simultaneously on the adsorbent. Thus the choice of regeneration procedure is important in ensuring proper release of the bound ions. For instance, metal oxides like iron (hydr)oxides bind phosphate via a ligand exchange mechanism with their surface hydroxyl groups (Cornell and Schwertmann 2004). Their regeneration requires using an alkaline solution to reverse the reaction and release the bound phosphate (Kalaitzidou et al. 2016). However, an earlier study showed surface precipitation on iron oxide adsorbents used in a drinking water matrix and an additional step using acidic solution was required to regenerate the adsorbents (Kunaschk et al. 2015). Moreover, regeneration first with an acidic solution before using alkaline solution improved the adsorbent reusability compared to the reverse order. This was attributed to surface precipitates blocking the adsorbed phosphate and hence the need to first remove the surface precipitates before desorbing the phosphate.

In the current study, we use a similar regeneration approach to optimize phosphate adsorbents in municipal wastewater effluent. We used commercially available iron (hydr)oxide based adsorbents since iron oxides have been known for their good phosphate adsorption properties (Cornell and Schwertmann 2004). These were granular ferric hydroxide (GEH), Ferrosorp (FSP), and an ion exchange resin impregnated with iron oxide (BioPhree). GEH and FSP are porous iron oxides chosen for their high surface area. The BioPhree (henceforth referred as IEX) is similar to a hybrid ion exchange resin where the iron oxide is responsible for the phosphate adsorption and the resin acts as a backbone matrix (Blaney et al. 2007). Two principal factors of an adsorbent govern the process economics: i) Its adsorption capacity (at a given effluent concentration and under a given operation time) ii) its reusability. During the course of the experiments, we focused on improving both these properties. The regeneration procedure used included an alkaline solution to desorb phosphate as well as an acidic solution to remove surface precipitates. The order of using these solutions was also varied during regeneration to understand the effect on reusability. Moreover, adsorbent properties (like surface area and crystallinity) and mass balances of competing ions were monitored during the different adsorption-regeneration cycles. Finally, to test adsorbent regeneration from a practical viewpoint, a regeneration process with a minimal number of steps and chemical consumption was done. The methods were aimed at monitoring the adsorbents to develop the best practices to regenerate and reuse the adsorbents.

2. Materials and methods

2.1. Chemicals

Potassium dihydrogen phosphate (KH_2PO_4), hydrochloric acid (HCl) and sodium hydroxide (NaOH) were obtained from VWR chemicals. The adsorbents: granular ferric hydroxide (GEH), Ferrosorp (FSP) and ion exchange resin impregnated with iron oxide (commercially called BioPhree, but referred to as IEX henceforth) were provided by GEH Wasserchemie Gmbh, HeGO Biotech Gmbh, and Green Water Solution, respectively.

2.2. Methods

2.2.1. Wastewater effluent

Wastewater effluent was sampled from Leeuwarden wastewater treatment plant and spiked using KH_2PO_4 to get an initial phosphate concentration around 2 mg P/L. No other chemicals were spiked. The particulates in the wastewater effluent were separated by sedimentation and only the supernatant was used for the adsorption runs. Phosphorous analysis of filtered (using 0.45 µm membrane filter) and unfiltered supernatant showed that there was no particulate phosphorus larger than 0.45 micron present in the supernatant.

2.2.2. Adsorbent columns

Adsorbents GEH and FSP were ground and sieved to reach particle size ranges of 1 to 1.25 mm and 0.25 to 0.325 mm, respectively. IEX was by default delivered (in its wet state) in the particle size range between 0.25 to 0.325 mm. The adsorbents were filled inside a glass column (height = 20 cm, diameter =

1.8 cm) to get an adsorbent bed volume of 10 ± 0.5 ml. The adsorbent bed was packed by using glass wool and glass beads to fill the remaining volume of the column (fig S1 in supporting information shows the adsorbent column).

2.2.3. Adsorption and regeneration experiments

For the adsorption experiments, the wastewater effluent was pumped to the adsorbent columns in an upflow mode with a flowrate of 2 ml/min. This gave an empty bed contact time (EBCT) of 5 minutes. The treated solution from the outlet of the column was collected in an automated fraction collector every 3 to 5 hours. These were analyzed for phosphate and the adsorption process was stopped when the outlet phosphate concentration reached 0.1 mg P/L.

Adsorbent regeneration was done in different ways. The first method, designated as alkaline-acid regeneration, used an alkaline solution followed by an acidic solution. The second method, designated as acid-alkaline regeneration, used acidic solution followed by alkaline solution. In both these methods, the acid wash was done till the pH coming out of the column matched the initial pH of the acid solution. Moreover the pH in the adsorbent column was neutralized with distilled water or HCl solution of pH 4 prior to subsequent adsorption cycles. Finally, in another method, the adsorbent was regenerated only with alkaline solution and the pH in the adsorbent column was not neutralized prior to subsequent adsorption cycles. Table 1 summarizes the different regeneration methods used. For all methods, 3 adsorption and regeneration cycles were done. The GEH and FSP adsorbent particle sizes were varied to check the influence on the adsorption capacity, whereas the IEX was only available in the size range of 0.25 to 0.325 mm. The rationale for varying the acid wash conditions in different regeneration cycles was to improve the reusability. The terms alkaline desorption and acid wash are used in the text to imply release of ions from the adsorbent using alkaline and acidic solution respectively.

Table 1: Differences in the regeneration methods

Regeneration method	**Adsorbents used**	**Particle size (mm)**	**Regeneration conditions**
Alkaline-acid regeneration	GEH, FSP	1 to 1.25	Alkaline desorption – For all 3 cycles: 100 ml of 1 M NaOH, Recirculation mode for 24 h, Flowrate = 5 ml/min; Acid wash - For all 3 cycles: Single pass mode with HCl (pH = 4) till outlet pH reached 4, Flowrate= 2 ml/min
Acid-alkaline regeneration	GEH, FSP, IEX	0.25 to 0.325	Acid wash – 1st cycle: Recirculation mode with 1L HCl (pH = 4), HCl was added to the acid reservoir till pH stabilized at 4. 2nd and 3rd cycle: HCl (pH = 2.5), Single pass mode till outlet pH reached 2.5, Flowrate = 2ml/min; Alkaline desorption – For all 3 cycles: 100 ml of 1 M NaOH, Recirculation mode for 24 h,

			Flowrate = 5 ml/min
Alkaline regeneration	FSP	0.25 to 0.325	<u>Alkaline desorption</u> For all 3 cycles: 100 ml of 1 M NaOH, Recirculation mode for 24 h, Flowrate = 5 ml/min

2.2.4. Analysis of wastewater samples

Calcium, magnesium, nitrate, nitrite, phosphate and sulphate ions were analyzed by ion chromatography (Metrohm Compact IC Flex 930). Soluble phosphorous, silicon, and iron were measured using inductively-coupled plasma optical emission spectroscopy (Perkin Elmer, Optima 5300 DV). Dissolved organic carbon and inorganic carbon (carbonate ion) were measured using combustion catalytic oxidation method with TOC analyzer (Shimadzu, TOC-L CPH). Table 2 shows the composition of the wastewater effluent used.

Table 2: Wastewater effluent (from Leeuwarden) characteristics:

Components/Parameters	**Average value/concentration**
Temperature (during adsorption)	21 °C
pH	7.9 ± 0.2
Conductivity	1.8 ± 0.2 mS/cm
Calcium	66 ± 5 mg Ca/L
Magnesium	17 ± 0.5 mg Mg/L

Nitrate	5.5 ± 1 mg NO_3^-/L
Nitrite	2.5 ± 2 mg NO_2^-/L
Phosphate (after spiking)	2 ± 0.2 mg P/L
Soluble silicon	12 ± 1.5 mg Si/L
Sulphate	31 ± 1 mg SO_4^{2-}/L
Dissolved organic carbon	18 ± 1 mg C/L
Inorganic carbon	106 ± 3 mg C/L

2.2.5. Adsorbent characterization

The types of iron oxide in the adsorbents were determined using Mössbauer spectroscopy. Transmission ^{57}Fe Mössbauer spectra were collected at different temperatures with conventional constant acceleration and sinusoidal velocity spectrometers using a ^{57}Co (Rh) source. Velocity calibration was carried out using an α-Fe foil. The Mössbauer spectra were fitted using the Mosswinn 4.0 program.

For determining the surface area of the adsorbents, nitrogen adsorption and desorption cycles were carried out using Micromeritics TriStar 3000. The data from the nitrogen adsorption-desorption profiles were fitted with models included in the analysis software to obtain the pore area from Non Local Density Functional Theory (NLDFT) (Cracknell et al. 1995).

The elemental composition of the adsorbents was quantitatively measured by microwave digestion with 67 % HNO_3. The elemental distribution on the adsorbent surface was monitored using scanning electron microscope coupled energy dispersive X-Ray (SEM-EDX). The imaging was done using a JEOL JSM-6480 LV Scanning Electron Microscope. Elemental analysis was done at an acceleration voltage of 15 kV using Oxford Instruments x-act SDD Energy Dispersive X-ray Spectrometer. The composition of the surface precipitates on the adsorbent was determined using Raman Spectroscopy (LabRam HR Raman spectrometer).

Point of zero charge (PZC) of the adsorbents was determined by using the salt addition method (Mahmood et al. 2011); 0.2 g of adsorbents (particle size < 0.35 mm) were added to aqueous solutions of 0.1 M $NaNO_3$ with initial pH varying from 4 to 11. The $NaNO_3$ solution was bubbled with N_2 gas prior to the adsorbent addition, and the experiment was conducted in a glovebox with N_2 atmosphere to avoid effect of carbon dioxide on the pH. The adsorbents were allowed to mix for 48 hours and the final pH was measured. The difference in initial and final pH was plotted against the initial pH values and the PZC was defined by the pH where the difference in pH was zero. Table 3 shows the characteristics of the adsorbents used.

Table 3: Adsorbent characteristics

Adsorbent	**Type of adsorbent**	**Bulk density (g/cm^3)**	**Surface area (m^2/g)**	**Point of zero charge**	**Major constituents (wt%)[a]**
GEH	Porous iron oxide	1.1	244	6.1	Fe – 51 %
FSP	Porous iron oxide	0.7	179	9.1	Fe – 47 %, Ca – 8 %
IEX[b]	Iron oxide impregnated in resin	0.7	58	6.6	Fe – 22 %, TOC – 25 %

[a]- Shows constituents comprising more than 5 wt % of adsorbent as measured after microwave digestion of the samples

[b] – For the IEX the bulk density was measured in its default wet state, whereas for FSP and GEH the bulk density was estimated in their dry forms.

2.2.6. Estimation of adsorption capacity

The phosphate adsorption capacity was calculated by evaluating breakthrough curves for the different adsorbents. The breakthrough point was considered to be the point when the outlet phosphate concentration from the columns reached 0.1 mg P/L. The detection limit for phosphate was 0.02 mg P/L. The amount of phosphate adsorbed was calculated by plotting the concentration of phosphate removed versus the volume of solution passed and estimating the area under the curve using trapezoidal rule (Atkinson 1989).

3. Results and discussion

3.1. Optimization of phosphate adsorption and reusability by varying adsorbent particle size and regeneration conditions

Fig 1 shows the phosphate adsorption capacities of GEH and FSP for 3 consecutive cycles using alkaline-acid regeneration. The adsorption capacity was estimated from the breakthrough curves when the phosphate concentration from the column outlet reached 0.1 mg P/L (fig S2 in supporting information shows an example of such breakthrough curve).

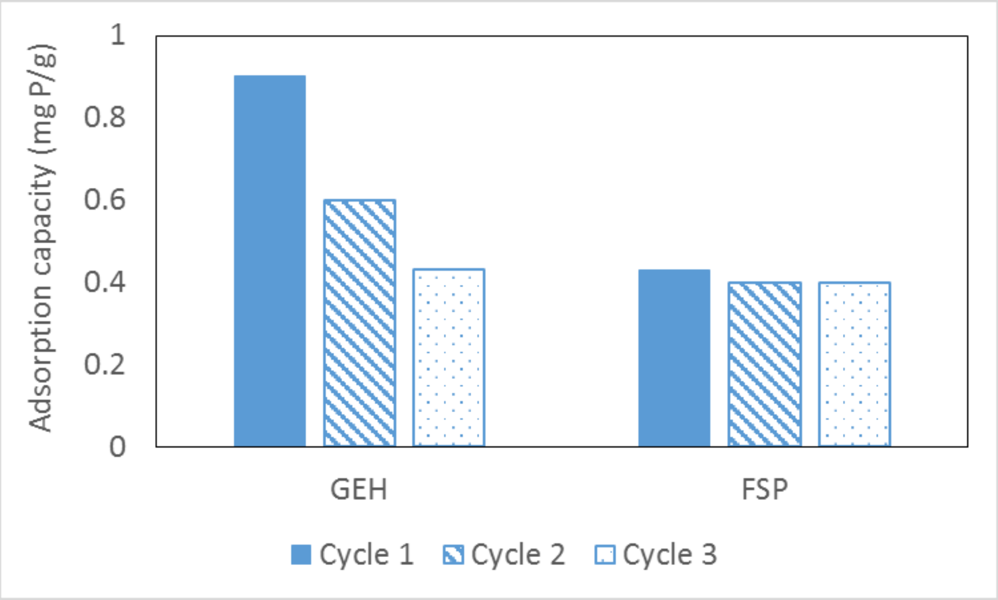

Fig 1: Adsorption capacities of 1 to 1.25 mm sized GEH and FSP for breakthrough at 0.1 mg P/L using alkaline-acid regeneration

Fig 1 shows that for the 1st cycle, the adsorption capacity of GEH and FSP at effluent concentration of 0.1 mg P/L was around 0.9 and 0.4 mg P/g, respectively. A phosphate molecule has a diameter of 0.48 nm (Tawfik and Viola 2011). Assuming a monolayer coverage, these adsorption capacities correspond to an area of 3.1 m^2 for GEH and 1.4 m^2 for FSP. This implies only around 1 % of the overall surface area is covered in both these adsorbents. It must be noted that the values shown in fig 1 are not equilibrium adsorption capacities, but adsorption capacities estimated under the given EBCT of 5 minutes. The reason for such a low adsorption capacity corresponding to a very low area coverage fraction is likely due to the diffusion limitation in these porous adsorbents.

Moreover, the reusability of GEH was also affected significantly during these 3 cycles. The adsorption capacity for GEH dropped by 50 % by the 3rd cycle, whereas for FSP the adsorption capacity dropped by about 7 %.

To improve the reusability of the adsorbents, the regeneration order was reversed by first doing an acid wash followed by alkaline desorption as suggested elsewhere (Kunaschk et al. 2015). To improve the adsorption capacity of the adsorbents, GEH and FSP were grinded to a particle size of 0.25 to 0.325 mm, which was similar to the particle size of the IEX adsorbent. Fig 2 shows the phosphate adsorption capacities of GEH, FSP and IEX for 3 consecutive cycles using acid-alkaline regeneration.

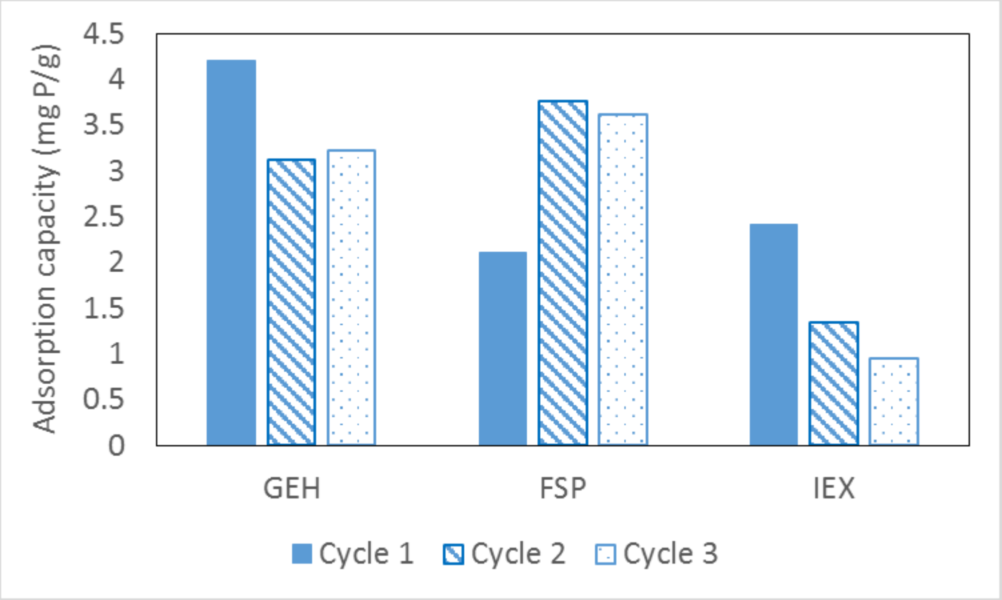

Fig 2: Adsorption capacities of 0.25 to 0.325 mm sized GEH, FSP and IEX for breakthrough at 0.1 mg P/L using acid-alkaline regeneration

Phosphate adsorption capacities for the 1st cycle of GEH and FSP were more than 4 times higher for the 0.25 to 0.325 mm sized particles as compared to the 1 to 1.25 mm sized particles. The specific surface areas of the large (1 to 1.25 mm) and small (0.25 to 0.325 mm) sized adsorbents were similar (table S1). GEH and FSP are porous adsorbents where the measured surface area is related to micropores (< 2 nm) and mesopores (2 to 50 nm) (as per the NLDFT method) (Cracknell et al. 1995). Thereby grinding them in the mm range does not change their overall area. Porous adsorbents offer the advantage of high surface area even in granular form, thereby allowing for easier handling and operation. However, the porous nature of such adsorbents implies that the adsorption is limited by diffusion. Thereby, under non-equilibrium conditions, decreasing their particle size increases the phosphate adsorption even though their surface area stays the same (fig 1 and fig 2). This shows the need to consider the accessibility of the pores properties while designing such adsorbents, especially for operations with short contact times.

The reusability of the GEH and FSP adsorbents were enhanced for the smaller particle sizes. The decrease in adsorption capacity of GEH for the 2nd and 3rd cycles in figure 2 was less than the decrease seen in fig 1. The adsorption capacity of FSP increased for the 2nd and 3rd cycles by a factor 2 as compared to cycle 1. The adsorption capacity of IEX decreased by 50 % by the 3rd cycle.

Usually the reusability of adsorbents in lab scale experiments are demonstrated for 5 to 10 cycles (Chitrakar et al. 2006, Kim et al. 2017, Wan et al. 2016). However, as can be seen from fig 1 and fig 2, we see interesting trends in reusability of the adsorbents already by 3 cycles. This is also due to the complex nature of the wastewater effluent as opposed to the cleaner solutions spiked with phosphate that are often used to demonstrate successful reusability. Thus the focus of this study henceforth was to understand the reason for these differing trends in reusability. By understanding what factors exactly contribute to adsorbent reusability, the optimal procedures for regeneration can be designed. Even if 5 to 10 cycles of successful reuse can be demonstrated via the optimal regeneration methods and if it can be shown that the adsorbent characteristics do not change over this period, then the adsorbent lifetime can be extrapolated to longer reuse cycles.

3.2. Understanding phosphate adsorption and reusability by monitoring different parameters

3.2.1. Effect of surface (porous) area

During the regeneration process the acid and alkaline treatment might cause the iron oxides to solubilize and recrystallize. In such a case the physical as well as chemical properties of the iron oxide can change, such as the change in surface area or the crystallinity/type of iron oxide. A change in surface area could lead to a loss of active sites which would thus affect the adsorbent reusability. Table 4 shows the overall change in adsorbent surface area along with the change in adsorption capacity for cycle 1 and cycle 3 (raw data in table S1 in supporting information).

Table 4: Overall change in surface area (between 1st and 3rd cycles) for adsorbents regenerated using the alkaline-acid and acid-alkaline methods. The + and – signs imply increase or decrease.

	Regeneration using alkaline-acid method		**Regeneration using acid-alkaline method**	
Adsorbents	**Change in surface area**	**Change in adsorption capacity**	**Change in surface area**	**Change in adsorption capacity**
GEH	- 10 %	- 52 %	- 8 %	- 23 %
FSP	+ 25 %	- 7 %	+ 56 %	+ 71 %
IEX			+ 20 %	- 60 %

In general, except for FSP regenerated using the acid-alkaline method, the change in surface area did not show a correlation with the change in adsorption capacity. This implies that the adsorbent reusability is also affected by other parameters.

3.2.2. Effect of the type of iron oxide in the adsorbent

Phosphate adsorption happens on iron oxides via a ligand exchange mechanism with the surface hydroxyl groups (Parfitt et al. 1975). The change in the crystallinity/type of iron oxide during regeneration will lead to exposure of differing types and amount of surface hydroxyl groups which in turn will affect the phosphate adsorption (Cornell and Schwertmann 2004). In an earlier study, a decrease in crystallinity of goethite decreased the adsorbent reusability within 2 cycles (Chitrakar et al. 2006). The crystallinity of akaganeite stayed intact in the same study and the adsorbent could be reused successfully for 10 cycles. Apart from the regeneration chemicals, the binding of ions like silicate and organics from the wastewater can also influence the crystallinity of the adsorbents (Schwertmann et al. 1984).

To measure if the type of iron oxide changes during the adsorbent usage, the adsorbents were measured with Mössbauer spectroscopy in their unused states and used state (after 3 adsorption cycles). During these cycles the adsorbents were regenerated using the acid-alkaline method which involved acid wash at pH 2.5 and alkaline desorption at pH 14. Table 5 shows the Mössbauer fitted parameters for the different adsorbents.

Table 5: The Mössbauer fitted parameters of different adsorbents in their unused and used states. Used state refers to the adsorbent after 3 adsorption cycles.

Sample	*T (K)*	*IS* $(mm\cdot s^{-1})$	*QS* $(mm\cdot s^{-1})$	*Hyperfine field (T)*	*Γ* $(mm\cdot s^{-1})$	*Phase*	*Spectral contribution (%)*
GEH	4.2	0.35	0.06	51.6	0.45	Fe^{3+} (*Hematite*)	11
		0.35	-0.08	47.5*	0.44	Fe^{3+} (*Ferrihydrite*)	89
GEH used	4.2	0.36	0.02	51.9	0.45	Fe^{3+} (*Hematite*)	10
		0.35	-0.07	47.8*	0.45	Fe^{3+} (*Ferrihydrite*)	90
FSP	4.2	0.33	-0.01	44.6*	0.53	Fe^{3+} (*Ferrihydrite)*	100

FSP used	4.2	0.34	-0.01	48.0*	0.44	Fe^{3+} (*Ferrihydrite*)	100
IEX	4.2	0.36	-0.15	50.6	0.39	Fe^{3+} (*Goethite/Hematite*)	21
		0.36	0.11	52.8	0.45	Fe^{3+} (*Hematite*)	7
		0.35	-0.10	46.3*	0.42	Fe^{3+} (*Ferrihydrite*)	72
IEX used	4.2	0.36	-0.10	50.2	0.49	Fe^{3+} (*Goethite/Hematite*)	31
		0.35	0.01	52.0	0.36	Fe^{3+} (*Hematite*)	8
		0.35	-0.08	46.7*	0.45	Fe^{3+} (*Ferrihydrite*)	61

Experimental uncertainties: Isomer shift: I.S. ± 0.01 mm s^{-1}; Quadrupole splitting: Q.S. ± 0.01 mm s^{-1}; Line width: Γ ± 0.01 mm s^{-1}; Hyperfine field: ± 0.1 T; Spectral contribution: ± 3%. *Average magnetic field.

Based on the fitted parameters (Murad 1988), table 5 shows that ferrihydrite is present in all the samples. GEH and IEX comprised of more than one type of iron oxide. The spectral contribution of the different iron oxide phases shows the transformation between used and unused adsorbents. For instance GEH does not undergo significant changes in its composition before and after adsorption. It must be noted that GEH has previously been reported as akaganeite when analyzed using X-ray diffraction (XRD)(Kolbe et al. 2011). But XRD detects only the crystalline part of the adsorbent whereas Mossbauer spectroscopy can detect even the amorphous/nanocrystalline iron oxides making it a more suitable method.

For FSP even though the iron oxide phase is ferrihydrite in both the used and unused samples, there is a change in the hyperfine field. The unused FSP has a hyperfine field that is lower than the usual value for ferrihydrite (Murad 1988, Murad; and Schwertmann 1980). It could be that the FSP transformed from an adsorbent having a highly disordered to a more ordered ferrihydrite species. Usually the surface area is higher for more amorphous iron oxides (Borggaard 2006). However in this case the used FSP, i.e. the adsorbent having more crystalline ferrihydrite, showed a higher surface area (table S1). The surface area of the used FSP increased by more than 56 % compared to the unused FSP. This could be the reason for the increased adsorption capacity of the FSP after regeneration by the acid-alkaline method. But this increase in surface area need not have been due to the transformation of iron oxide species but rather due to the removal of surface precipitates as will be discussed later.

For IEX, the content of ferrihydrite decreased and the overall content of goethite/hematite increased by 10 %. This higher transformation of the iron oxide phase in the IEX compared to GEH and FSP could be due to the nature of iron distribution in the adsorbent. FSP and GEH are bulk iron oxides, whereas IEX is a resin impregnated with iron oxide nanoparticles. This means that the iron oxide particles in IEX have a higher surface area to volume ratio. Thus the fraction of the total iron oxide that is accessible to phosphate adsorption will be much higher in the IEX as compared to FSP and GEH. Hence, even if the active sites in all the adsorbents underwent similar transformation during regeneration, the overall change in iron oxide phase will be higher for the IEX. Goethite and hematite have lower phosphate adsorption per unit area compared to ferrihydrite (Wang et al. 2013). So it is possible that this transformation in the IEX contributes to decrease in its reusability. However the decrease in ferrihydrite content is only 11 % whereas the decrease in adsorption capacity is about 60 %. Thus it can be understood that transformation of the iron oxides alone is not affecting the reusability.

3.2.3. Effect of competing ions

To make the adsorbent reusable, it is necessary to regenerate the adsorbent properly, whereby the adsorbate molecules are desorbed, and the active sites are replenished. The phosphate adsorption experiments with 1 to 1.25 mm sized GEH and FSP granules were used to optimize the adsorption and regeneration procedure. Apart from phosphate, different competing ions were monitored during adsorption cycle 1. Based on these observations (shown in fig S3), selected ions were screened to be included in a mass balance while using adsorbents with particle size 0.25 to 0.325 mm. These included calcium, organic carbon, inorganic carbon, silicon.

Values of the mass balance for the 0.25 to 0.325 mm sized adsorbents are shown in table S2 in the supporting information. The mass balances could not be closed in several cases. For e.g. for GEH, the silicon released during regeneration was always lower than the amount adsorbed, and for IEX, the dissolved organic carbon released was always lower than amount adsorbed (shown in fig S4).

Calcium was monitored since it can form surface precipitates (Kunaschk et al. 2015). The release of calcium from the different adsorbents regenerated using the acid-alkaline regeneration is shown in fig S4. For GEH, the calcium release was less than 50 % in cycle 1. Thus the acid wash was switched from a pH of 4 to pH of 2.5 for cycles 2 and 3, based on the earlier protocol (Kunaschk et al. 2015). This improved the calcium release significantly amounting to 98 and 88 % for cycles 2 and 3. Iron concentration was monitored in the acid wash to check if the adsorbent was leaching iron. Even using a pH as low as 2.5, the amount of iron released per cycle for all the adsorbents was less than 0.01 % of the adsorbent mass packed in the column. For FSP, the calcium release during cycle 1 and 2 was higher than 100 % since FSP by default consists of calcium (see table 3). For IEX, only around 20 % of calcium could be released during cycles 2 and 3.

In this study, the alkaline desorption step was used to desorb ions like phosphate that bind with the surface hydroxyl groups on the iron oxide. The acid wash step on the other hand was used to release the surface precipitates. Thus the release of a competing ion in either the acid wash step or during alkaline desorption gives information about its mechanism of binding on the adsorbent.

Fig 3 shows the average relative release percentages of different ions for FSP during acid wash and alkaline desorption while using the acid-alkaline regeneration. The adsorbents GEH and IEX exhibited similar release patterns for the different ions (fig S5).

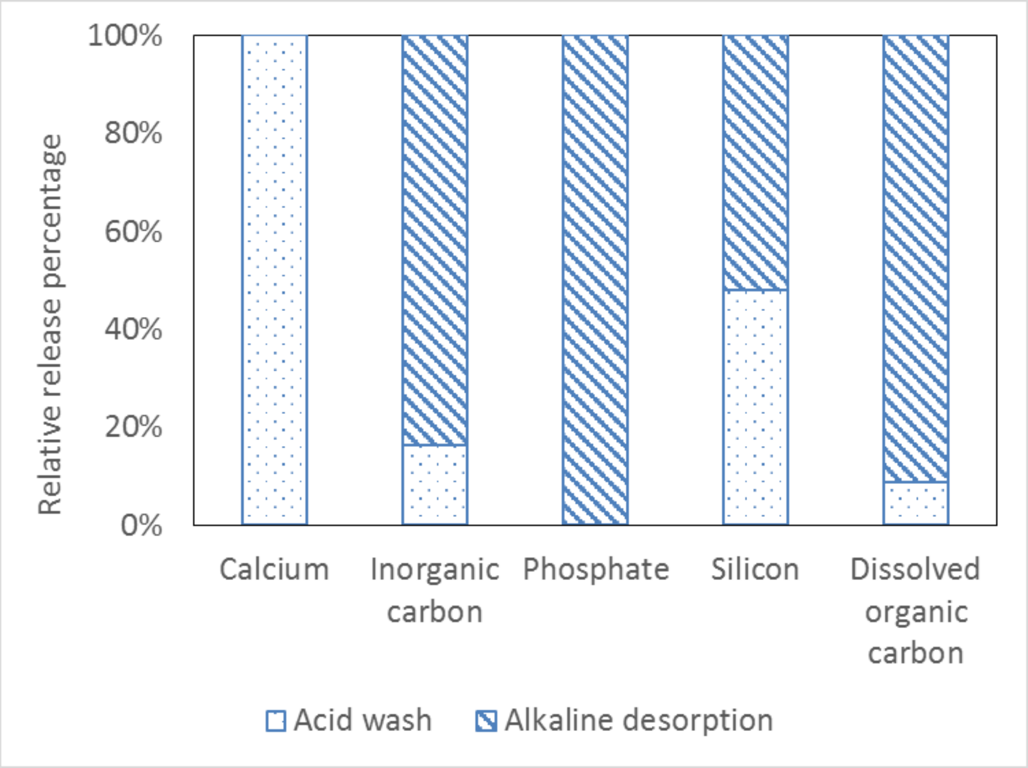

Fig 3: Relative release percentage of different ions from FSP in acid wash and alkaline desorption (for acid-alkaline regeneration)

From fig 3, it can be seen that calcium is released exclusively during acid wash whereas phosphate is released exclusively via alkaline desorption. This was the case for all adsorbents (fig S5). This shows that there is no formation of calcium phosphate precipitate and these ions bind via different mechanisms.

A majority of the inorganic carbon, which at this pH would represent (bi)carbonate ions, was released during alkaline desorption. While it is possible that carbonate ions can sometimes adsorb via ligand exchange on iron oxides (Chunming Su and Suarez 1997), it was expected that in this case carbonate forms surface precipitates with calcium. But in these experiments the acid wash was done in an open system. Therefore, if there were carbonate ions that were released during the acid wash, they would have mostly escaped as carbon dioxide (Hey et al. 1994).

Soluble silicon was about equally released in acid wash as well as in alkaline desorption. Silicon present as orthosilicates can bind as innersphere complexes that would be desorbed during alkaline desorption, but could also form calcium silicate based precipitates that would dissolve in the acid wash (Lothenbach and Nonat 2015, Sigg and Stumm 1981). Organic carbon was mostly released by alkaline desorption. This is expected since organics like humics also bind to iron oxides via the ligand exchange with their surface functional groups (Antelo et al. 2007, Ko et al. 2005).

These results shows that different ions bind on the adsorbent via different mechanisms and not all of them are completely released. More regeneration cycles would show how this affects the adsorbent reusability over time.

3.2.4. Effect of calcium based surface precipitation

The reason for using acid wash in the regeneration methods was based on the premise of removing calcium based surface precipitates (Kunaschk et al. 2015). Fig 4 shows the SEM-EDX observations on the unused FSP, FSP that had been used for 3 adsorption cycles using acid-alkaline regeneration, and FSP that been used for 3 adsorption cycles but regenerated only using alkaline desorption. The color codes for the elemental maps are stated in the figure caption.

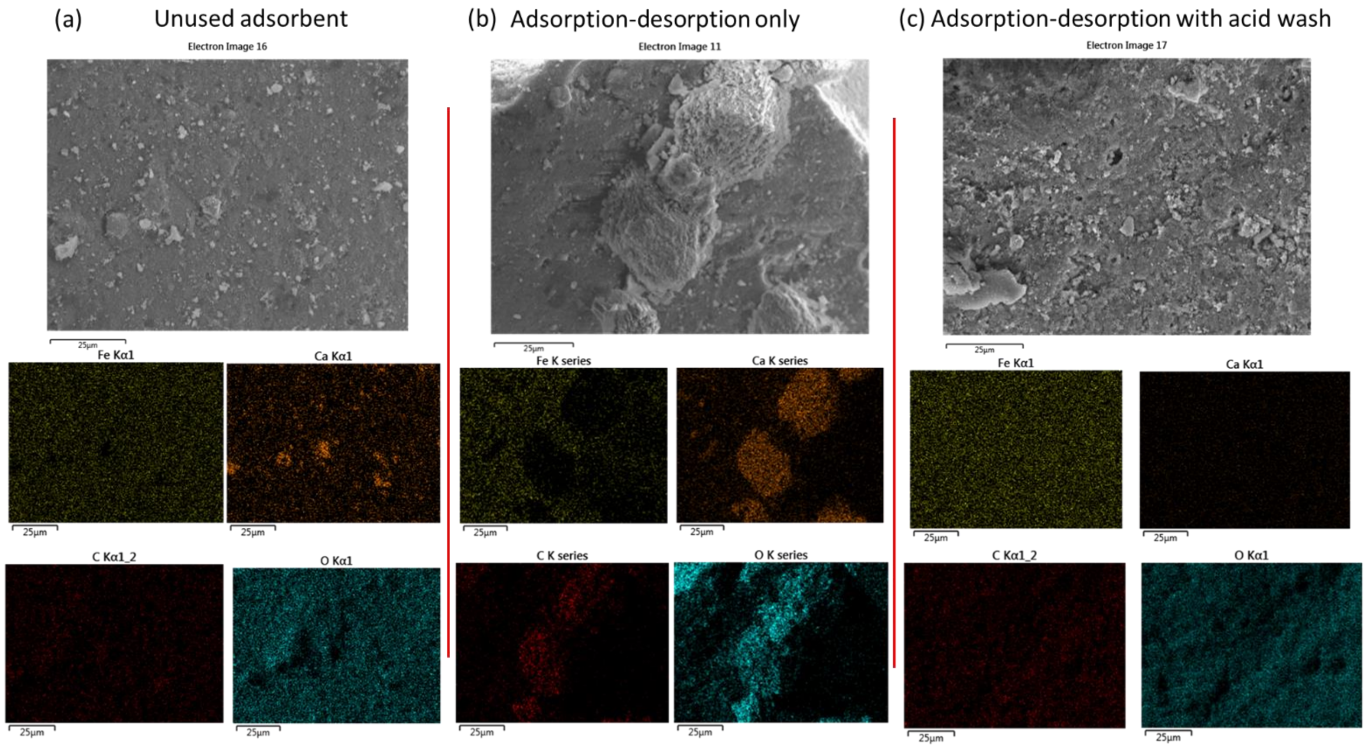

Fig 4: SEM-EDX observations of FSP adsorbent for (a) unused content (Ca content as per EDX = 5 wt %), (b) FSP regenerated without acid wash (Ca content = 15 wt %), (c) FSP regenerated with acid wash ash (Ca content = 0 wt %). Scalebar represent 25 µm. Color code for elemental maps- Yellow = Iron, Orange = Calcium, Red = Carbon, Blue = Oxygen.

It can be seen from fig 4 (a), that unused FSP has calcium by default. But the elemental map of calcium and carbon do not overlap implying there is no observable calcium carbonate. Fig 4 (b) shows the FSP that was regenerated only with alkaline desorption and no acid wash. There are large areas in the elemental distribution where calcium, carbon and oxygen overlap. This implies the presence of calcium carbonate. The observable calcium carbonate particles are about 25 µm in size. Fig 4 (c) shows that the acid washed FSP (using acid-alkaline regeneration) has no calcium left and thus the surface precipitates are removed via acid wash. This was confirmed by Raman spectroscopy where the FSP regenerated without acid wash showed Raman shift characteristics of calcium carbonate (shown in fig S6).

This result is in line with the observations in fig 3 and fig S5 that the calcium was released exclusively via the acid wash and hence must be present in the form of surface precipitates. While calcium carbonate was the only precipitate that was observable, some silicon was also released during the acid wash (fig 3), indicating the possibility of calcium silicate precipitates. However, the molar ratio of inorganic carbon to silicon present in the wastewater was more than 20 (as seen from table 2), and the solubility product for calcium carbonate is lower than calcium silicate (Benjamin 2010, Greenberg et al. 1960). Thus calcium carbonates are likely the dominant precipitates formed on the adsorbent surface.

To test for the effect of calcium based surface precipitates on the adsorbent reusability, the extent of calcium release from the adsorbents was correlated with the adsorption capacities. Fig 5 shows the change in phosphate adsorption capacity for a given cycle compared to the calcium released from the previous cycle. n+1 denotes the current cycle and n denotes the previous cycle.

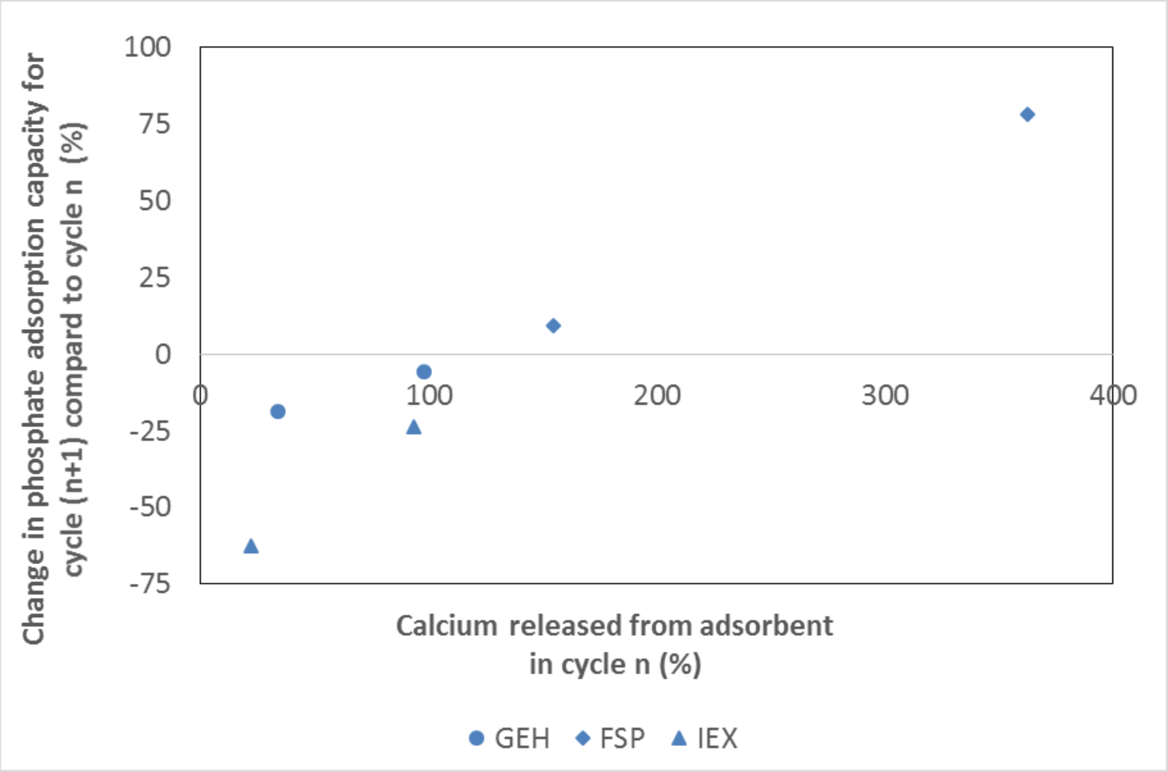

Fig 5: Change in phosphate adsorption capacity for a given cycle compared to the calcium release in the previous cycle (using acid-alkaline regeneration). n+1 is used to denote the current cycle and n denotes the previous cycle. n = 1,2. A negative change in the phosphate adsorption capacity implies the adsorbent reusability decreases whereas a positive change implies the reusability is enhanced.

Fig 5 includes data points from all the adsorbents regenerated using the acid-alkaline method. The data points showing more than 100 % calcium release are from FSP, since it contained calcium by default. The general trend observed is that the change in phosphate adsorption capacity is negative, i.e. the adsorbent reusability decreases, if not all the calcium from the adsorbent is released. This agrees with the reasoning that the calcium carbonate precipitates affect the adsorbent reusability and needs to be removed via an acid wash.

3.3. Mechanism of decrease in adsorbent reusability via surface precipitation

3.3.1. Hypothesis based on desorption of phosphate

The above results show the need for an acid wash step to remove the calcium based surface precipitates. As per the earlier study, having an acid wash step before alkaline desorption resulted in better adsorbent reusability than the other way around (Kunaschk et al. 2015). The explanation provided in that study was that adsorbed phosphate was blocked by surface precipitates. Thus the surface precipitates need to be first released before the phosphate can be released via alkaline desorption (a depiction of this hypothesis is shown in fig S7). This hypothesis was tested in our study by reversing the order of regeneration and checking the extent of phosphate released during regeneration. If the hypothesis is correct, then having an acid wash step after alkaline desorption should lead to a lower desorption of phosphate. Fig 6 (a) and (b) show phosphate released during alkaline desorption for the adsorbents used in the experiments corresponding to fig 1 and fig 2, respectively. The release percentage was calculated by measuring the amount desorbed in relation to the amount adsorbed.

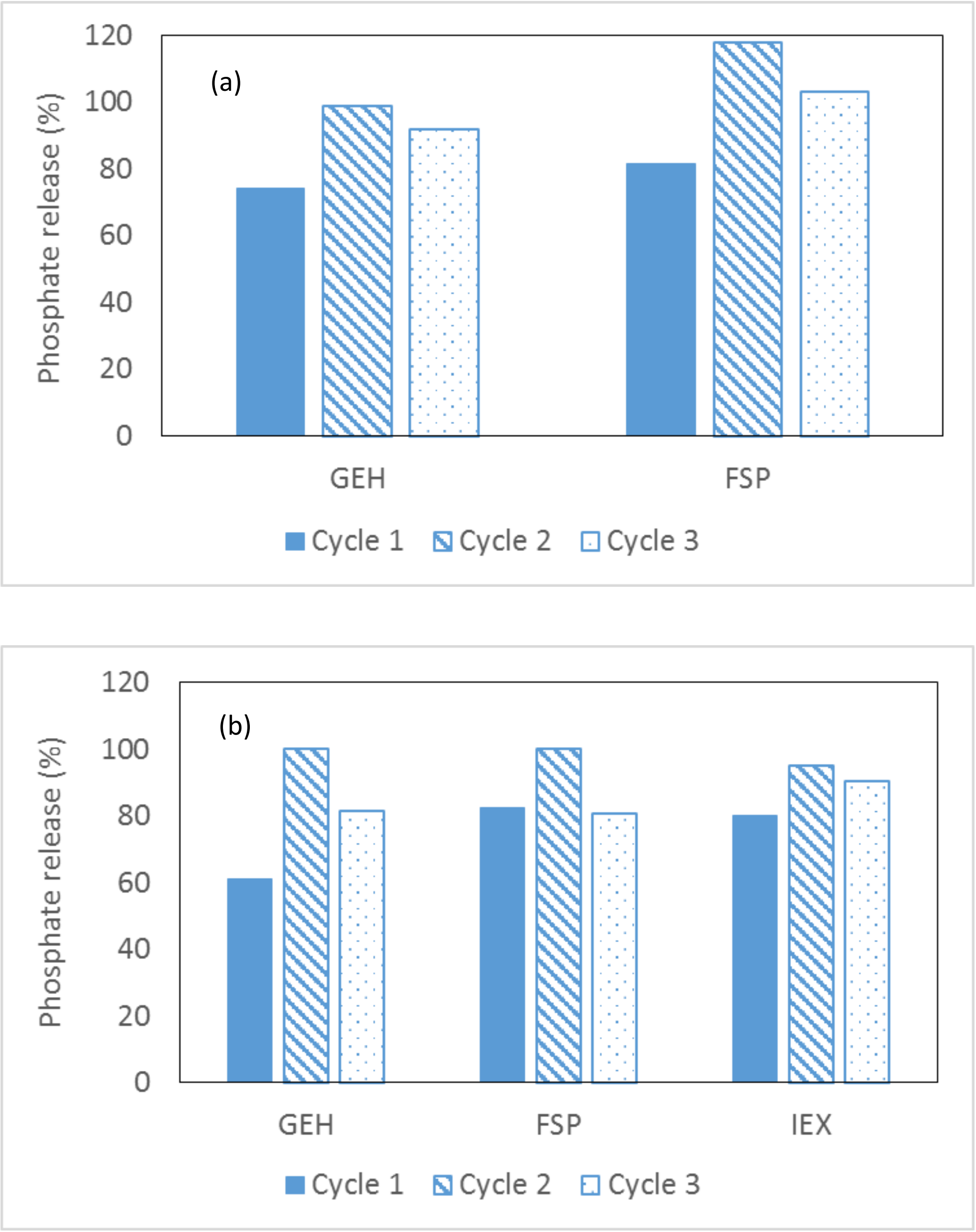

Fig 6: Percentage of phosphate released during alkaline desorption step using (a) alkaline-acid regeneration (b) acid-alkaline regeneration.

The phosphate release from all adsorbents mostly varied between 80 to 100 % using both regeneration methods. From fig 6 (a) it can be seen that FSP released more than 100 % phosphate for the 2nd cycle. This could have come from the phosphate that was not released during the 1st cycle. Comparing fig 6 (a) and 6 (b), there was no significant difference in the phosphate released by the two different regeneration methods. Thus, we conclude the differences in reusability as seen in fig 1 and fig 2 are apparently not due to blockage of adsorbed phosphate molecules as suggested in the earlier hypothesis.

This implies that the reason for differences in reusability for GEH and FSP between the two regeneration methods (as seen in fig 1 and fig 2) was due to the differences in the acid wash conditions. In the alkaline-acid regeneration, a pH of 4 was used for the acid wash step. This was to make sure iron dissolution from the iron oxides does not happen. In the acid-alkaline regeneration, we tried to improve the reusability by having stronger acid wash conditions. This was done by first having longer exposure time with pH 4. However, the calcium release from GEH was still less than 50 % (table S2 and fig S4). Thus a stronger acidic pH of 2.5 was used as suggested previously (Kunaschk et al. 2015). We noticed that no significant iron was leached from the acid wash implying that the acid was consumed primarily for breaking the surface precipitates. Thus the enhanced reusability was due to the release of surface precipitates. But apparently the surface precipitates do not hinder reusability by just blocking the adsorbed phosphate. This implies that there could be some additional mechanism by which surface precipitation affects reusability.

3.3.2. Possible role of calcium adsorption

It could be that the calcium based surface precipitates block the actives sites for phosphate on the adsorbent. However, as seen from fig 3 and fig S5, calcium binds on the adsorbent via a different mechanism to phosphate and hence should not directly block the active sites. In the case of FSP, the adsorbent already contains calcium in its unused state. If this calcium was present as precipitates blocking the adorbent pores or covering the iron oxide, the removal of this calcium during washing would expose active sites on the adsorbent that were previously inaccessible. This could be a reason for the increase in the surface area and the adsorption capacity of FSP for the 2nd and 3rd cycle when using acid-alkaline regeneration (fig 2).

Another possible way that calcium carbonate precipitates can affect the adsorbent reusability is by changing the point of zero charge (PZC) of the adsorbent and affecting the adsorption of calcium on them. Also, calcium ions are known to bind to iron oxide surfaces and enhance phosphate adsorption by making the surface electropositive (Antelo et al. 2015, Han et al. 2017, Rietra et al. 2001). A study testing GEH for adsorption of phosphonate, which binds to iron oxides in a similar mechanism as phosphate, reported that phosphonate adsorption at equilibrium doubled in a solution having a Ca:P molar ratio of 2 as compared to a solution without any calcium (Boels et al. 2012). This implies calcium adsorption onto GEH could result in a favorable equilibrium shift for phosphate adsorption as well.

Fig 7 shows the calcium and phosphate adsorption for all the adsorbents during all adsorption cycles for acid-alkaline regeneration. This includes only the calcium that was adsorbed during the adsorption process and does not consider the calcium that is by default in the FSP adsorbent. A positive correlation was observed between overall adsorption of calcium and phosphate ions.

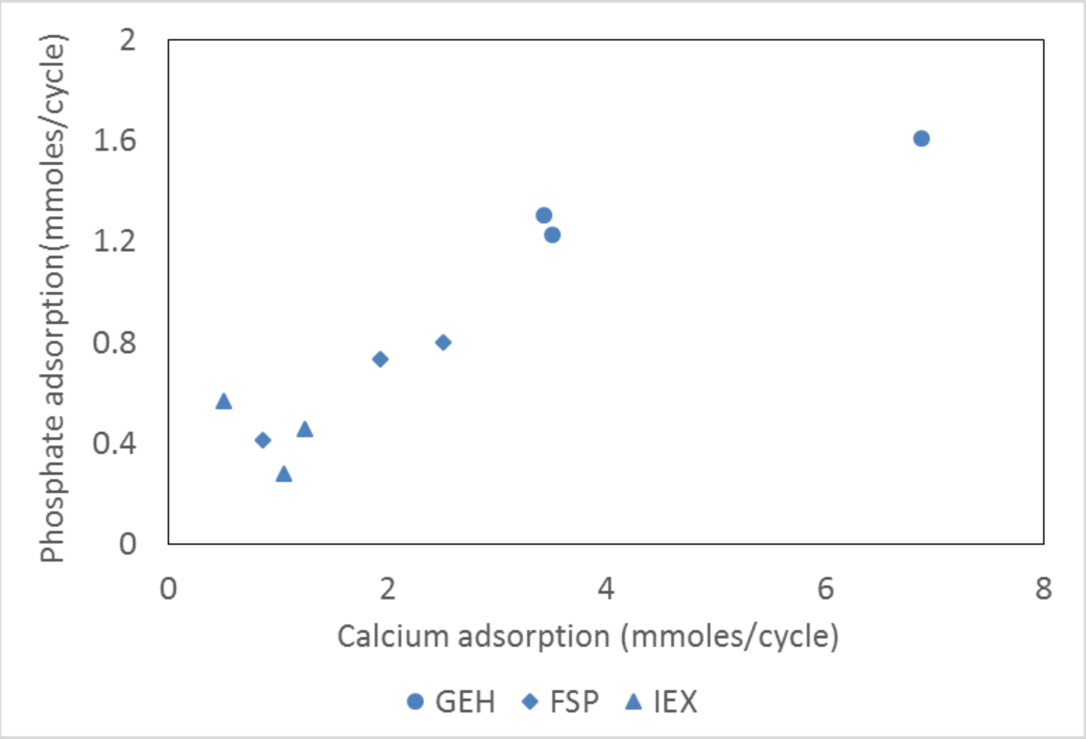

Fig 7: Correlation of Ca vs P adsorption (including all cycles for all adsorbents using acid-alkaline regeneration)

Calcium likely first physisorbs on the adsorbent surface before it forms calcium carbonate precipitates. Physisorption of calcium would enhance phosphate adsorption by making the surface electropositive (Antelo et al. 2015). Studies show that significant calcium binding happens only at a pH higher than the PZC of the adsorbent (Antelo et al. 2015, Rietra et al. 2001). At pH higher than PZC, the adsorbent surface is electronegative which will enhance calcium binding. Thus if an adsorbent has lower PZC than the pH of wastewater effluent, more calcium would bind to the adsorbent, which in turn would enhance the P adsorption. The pH of the wastewater effluent was 7.9 and the PZC for GEH and FSP was 6.1 and 9.1, respectively. This could be the reason why more calcium binds to GEH in cycle 1 compared to FSP (table S2 and fig S3). Hence GEH shows a higher phosphate adsorption capacity for cycle 1 than FSP.

However, the PZC on the adsorbent could shift upon the binding of calcium. Calcium carbonates have often shown PZC that are higher than 9 (Al Mahrouqi et al. 2017). The formation of calcium carbonate precipitates could thus increase the PZC of the adsorbent. This would usually be more favourable for phosphate adsorption since the adsorbent surface is more electropositive at a given pH. However, a higher PZC would mean less calcium adsorption, which in turn would imply less phosphate adsorption.

PZC measurements (fig S8) supported the above speculation. FSP with calcium carbonate had a higher PZC (PZC = 9.8), than the unused FSP which had some calcium (PZC = 9) and the acid-washed FSP which had no calcium (PZC = 7.5). These PZC's were determined using the salt addition method which depends on the pH measurements (Mahmood et al. 2011). This commonly used method can however have a shortcoming when measuring PZC of porous materials because impurities/unwashed ions (like hydroxide ions) in the pores can affect the measurement. Thus to prove/disprove this hypothesis, more accurate methods like zeta potential measurements should be used to determine surface charge.

For IEX, the correlation with calcium is not as strong. In the case of IEX, the decrease in reusability could thereby be due to multiple reasons like transformation of iron oxide phase and incomplete release of adsorbed organics. The incomplete release of organics from IEX could be related to the nature of regeneration. Hybrid ion exchange resins have been shown to remove anions via a combination of mechanisms involving ligand exchange on the iron oxide as well as coulombic interaction on the functional groups of the resin backbone (Sengupta and Pandit 2011). That study used a combination of sodium chloride (NaCl) and NaOH solutions for regeneration and reported ten successful regeneration cycles. However, the adsorption was studied for solutions containing only phosphate and sulphate ions unlike the wastewater effluent which also contains organics. Organics like humic acids also bind to hybrid ion exchange resins via the functional groups on the resin backbone as well as the iron oxides impregnated within them (Shuang et al. 2013). Hence regeneration with only NaOH might not release the organics bound on the functional groups of the resin. Although such organics might not compete with the active sites for phosphate directly, the binding of humics might confer a negative charge to the adsorbent (Antelo et al. 2007). This would be similar to a Donnan ion exclusion effect which would hinder the transport of anions into the resin and hence reduce phosphate adsorption in subsequent cycles (Cumbal and SenGupta 2005).

3.4. Adsorbent regeneration from a practical point of view

In regeneration methods involving acid wash, the pH in the adsorbent column was neutralized after the regeneration process. In some of these cases, when the alkaline desorption was the last step, more than 1000 bed volumes of distilled water were required to neutralize the column. To reduce the bed volume needed to neutralize the pH in these cases, the distilled water was spiked with HCl solution of pH 4.

In practice, a regeneration method producing minimal amount of waste and consuming the least chemicals should be employed. Moreover we also wanted to check if an acid wash was necessary prior to every adsorption cycle. In the current experiment, after alkaline desorption, the column was rinsed with 50 bed volumes of distilled water but the pH in the pores was still not neutralized. Subsequent adsorption runs were performed as such. Fig 8 shows the reusability of FSP when this regeneration strategy was used.

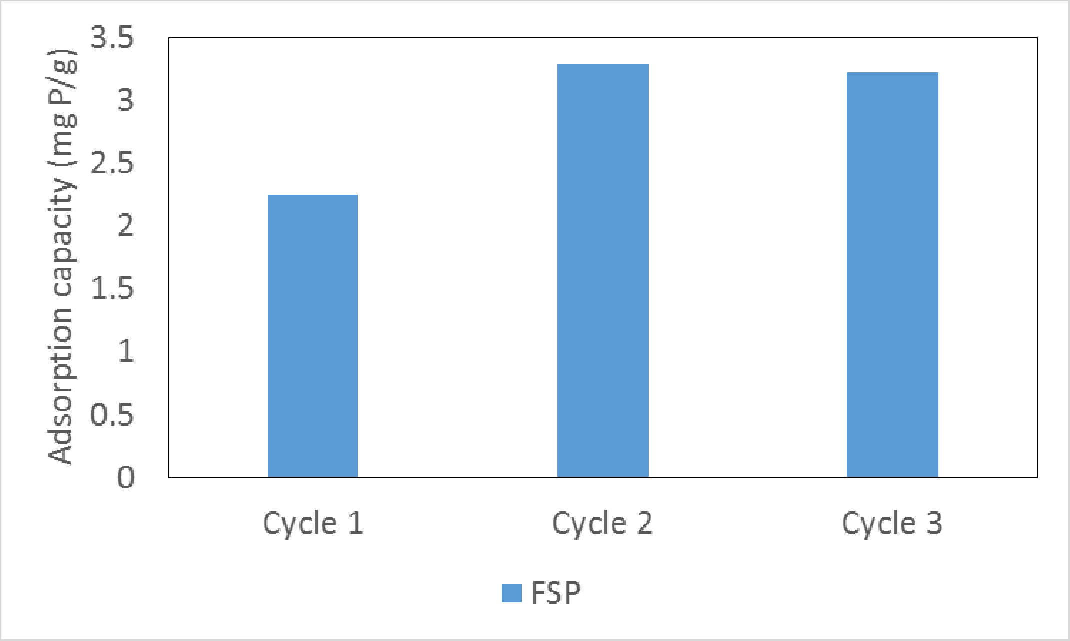

Fig 8: Adsorption capacity at effluent concentration of 0.1 mg P/L for FSP regenerated using only alkaline desorption. Adsorbent particle size was 0.25 to 0.325 mm.

Fig 8 shows that the phosphate adsorption capacity increased for cycle 2 and cycle 3. From mass balances (table S3), it was seen that amount of calcium bound to the adsorbent increased by a factor of about 7 times for cycles 2 and 3 compared to cycle 1. When comparing the pH profile from the column effluent with the calcium removal by the adsorbent, it was seen that the increase in calcium uptake coincided with higher effluent pH (fig S9).

The increase in calcium binding is likely because the pH inside the pores of the regenerated adsorbent is higher than the PZC. Thus a high amount of calcium could bind to the adsorbent in such cases, which could also enhance phosphate adsorption. During such a regeneration method there is also a possibility of calcium phosphate precipitation. This would happen in the initial bed volumes of the adsorption run where the pH is high. Results from mass balance calculations (table S3) show that the average phosphate release via alkaline desorption during this regeneration method is about 1.5 times lower than regeneration methods 1 and 2. This implies that some phosphate is bound as surface precipitates and hence this would be released only via acid wash. Thus an acid wash would probably be needed after some adsorption cycles.

Based on our observations, we can envision 3 different strategies for adsorbent regeneration as listed in table 6.

Table 6: Different regeneration strategies with their advantages and disadvantages

Regeneration method	**Advantages**	**Disadvantages**
Alkaline desorption with acid wash during every cycle	• Adsorption capacity is retained for each cycle • No buildup of surface precipitates after every cycle	• Neutralization of adsorbent bed required after every cycle • More chemical consumption during regeneration than other methods
Alkaline desorption each cycle, with intermittent acid wash in between some cycles	• Neutralization of adsorbent bed is not required after very cycle • Adsorption capacity will be retained for some cycles before adsorbent needs acid wash	• Calcium phosphate precipitation occurs • Part of phosphate will be release in acid wash
Alkaline desorption with no acid wash at all	• No acid consumption	• This is a viable option only if calcium

	- Least chemical consumption compared to other regeneration methods	carbonate precipitation does not happen - Phosphate adsorption capacity will be lower in the absence of calcium adsorption

In our study, we have used fresh acid and alkaline solutions for every regeneration step. In practice, the regenerate solutions would need to be reused to make the process more cost effective. We noticed that more than 250 bed volumes of acid wash solution of pH 2.5 were consumed while regenerating the FSP adsorbent. This would thus be attributed to waste generated during the regeneration process unless the solution can be reused over many cycles by only replenishing the acid consumed. One way to overcome this problem is to prevent surface precipitation in the first place and hence prevent an acid wash step, which is the 3rd type of regeneration strategy we highlight in table 6. To prevent/minimize surface precipitation, the mechanism of calcium binding needs to be understood better. Understanding this mechanism could help modify adsorbent properties such that calcium binding could be moderated. This can be used to enhance phosphate adsorption due to co-adsorption of calcium but minimize surface precipitation to lower acid consumption. For e.g. changing the adsorbent surface charge could be a strategy to moderate calcium binding.

Moreover, we have only shown 3 adsorption-regeneration cycles in our study. The adsorbent would need to last several adsorption cycles in practice. Hence future studies should also test the reusability over more adsorption-regeneration cycles.

4. Conclusion

This research has monitored various aspects that could affect the phosphate adsorption and reusability of adsorbents in a wastewater effluent.

- Despite having similar surface area, smaller adsorbent particles (0.25 to 0.325 mm) exhibited more than 4 times higher phosphate adsorption capacities than larger adsorbent particles (1 to 1.25 mm). This points at the importance of diffusion in porous adsorbents.
- In most cases only minor changes were noticed for the adsorbents in the type of iron oxide and surface area after 3 cycles of reuse. These changes were not significant to explain changes in reusability of the adsorbent.
- Reversing the order of acid wash and alkaline desorption steps during regeneration did not affect the desorption of phosphate during the 3 cycles.
- Calcium enhanced phosphate adsorption but also formed calcium carbonate based precipitates on the adsorbent which need to be removed to maintain reusability.
- Future studies should focus on understanding the mechanism of calcium binding and monitoring the reusability for more cycles.

5. Acknowledgements

This work was performed in the TTIW-cooperation framework of Wetsus, European Centre Of Excellence For Sustainable Water Technology (www.wetsus.nl). Wetsus is funded by the Dutch Ministry of Economic Affairs, the European Union Regional Development Fund, the Province of Friesland, the City of Leeuwarden and the EZ/Kompas program of the “Samenwerkingsverband Noord-Nederland”. We thank the participants of the research theme “Phosphate Recovery” for their financial support and helpful discussions.

6. References

Al Mahrouqi, D., Vinogradov, J. and Jackson, M.D. (2017) Zeta potential of artificial and natural calcite in aqueous solution. Advances in Colloid and Interface Science 240, 60-76.

Antelo, J., Arce, F., Avena, M., Fiol, S., López, R. and Macías, F. (2007) Adsorption of a soil humic acid at the surface of goethite and its competitive interaction with phosphate. Geoderma 138(1), 12-19.

Antelo, J., Arce, F. and Fiol, S. (2015) Arsenate and phosphate adsorption on ferrihydrite nanoparticles. Synergetic interaction with calcium ions. Chemical Geology 410, 53-62.

Atkinson, K. (1989) An Introduction to Numerical Analysis, Wiley.

Benjamin, M.M. (2010) Water Chemistry, Waveland Press, Incorporated.

Blaney, L.M., Cinar, S. and SenGupta, A.K. (2007) Hybrid anion exchanger for trace phosphate removal from water and wastewater. Water Research 41(7), 1603-1613.

Boels, L., Keesman, K.J. and Witkamp, G.J. (2012) Adsorption of phosphonate antiscalant from reverse osmosis membrane concentrate onto granular ferric hydroxide. Environ Sci Technol 46(17), 9638-9645.

Borggaard, O. (2006) Influence of iron oxides on the surface area of soil.

Cabrera, F., de Arambarri, P., Madrid, L. and Toga, C.G. (1981) Desorption of phosphate from iron oxides in relation to equilibrium pH and porosity. Geoderma 26(3), 203-216.

Chitrakar, R., Tezuka, S., Sonoda, A., Sakane, K., Ooi, K. and Hirotsu, T. (2006) Phosphate adsorption on synthetic goethite and akaganeite. Journal of Colloid and Interface Science 298(2), 602-608.

Chunming Su and Suarez, D.L. (1997) In situ infrared speciation of adsorbed carbonate on aluminum and iron oxides. Clays and Clay Minerals 45(6), 814-825.

Cordell, D., Drangert, J.-O. and White, S. (2009) The story of phosphorus: Global food security and food for thought. Global Environmental Change 19(2), 292-305.

Cornell, R.M. and Schwertmann, U. (2004) The Iron Oxides, pp. 253-296, Wiley-VCH Verlag GmbH & Co. KGaA.

Cracknell, R.F., Gubbins, K.E., Maddox, M. and Nicholson, D. (1995) Modeling Fluid Behavior in Well-Characterized Porous Materials. Accounts of Chemical Research 28(7), 281-288.

Cumbal, L. and SenGupta, A.K. (2005) Arsenic Removal Using Polymer-Supported Hydrated Iron(III) Oxide Nanoparticles: Role of Donnan Membrane Effect. Environmental Science & Technology 39(17), 6508-6515.

Greenberg, S.A., Chang, T.N. and Anderson, E. (1960) INVESTIGATION OF COLLOIDAL HYDRATED CALCIUM SILICATES. I. SOLUBILITY PRODUCTS. The Journal of Physical Chemistry 64(9), 1151-1157.

Han, C., Lalley, J., Iyanna, N. and Nadagouda, M.N. (2017) Removal of phosphate using calcium and magnesium-modified iron-based adsorbents. Materials Chemistry and Physics 198, 115-124.

Hey, M.J., Hilton, A.M. and Bee, R.D. (1994) The formation and growth of carbon dioxide gas bubbles from supersaturated aqueous solutions. Food Chemistry 51(4), 349-357.

Kalaitzidou, K., Mitrakas, M., Raptopoulou, C., Tolkou, A., Palasantza, P.-A. and Zouboulis, A. (2016) Pilot-Scale Phosphate Recovery from Secondary Wastewater Effluents.

Kim, M., Kim, H. and Byeon, S.H. (2017) Layered Yttrium Hydroxide l-Y(OH)3 Luminescent Adsorbent for Detection and Recovery of Phosphate from Water over a Wide pH Range. ACS Appl Mater Interfaces 9(46), 40461-40470.

Ko, I., Kim, J.-Y. and Kim, K.-W. (2005) Adsorption properties of soil humic and fulvic acids by hematite. Chemical Speciation & Bioavailability 17(2), 41-48.

Kolbe, F., Weiss, H., Morgenstern, P., Wennrich, R., Lorenz, W., Schurk, K., Stanjek, H. and Daus, B. (2011) Sorption of aqueous antimony and arsenic species onto akaganeite. Journal of Colloid and Interface Science 357(2), 460-465.

Kunaschk, M., Schmalz, V., Dietrich, N., Dittmar, T. and Worch, E. (2015) Novel regeneration method for phosphate loaded granular ferric (hydr)oxide – A contribution to phosphorus recycling. Water Research 71, 219-226.

L. Correll, D. (1998) The Role of Phosphorus in the Eutrophication of Receiving Waters: A Review.

Li, M., Liu, J., Xu, Y. and Qian, G. (2016) Phosphate adsorption on metal oxides and metal hydroxides: A comparative review. Environmental Reviews 24(3), 319-332.

Loganathan, P., Vigneswaran, S., Kandasamy, J. and Bolan, N.S. (2014) Removal and Recovery of Phosphate From Water Using Sorption. Critical Reviews in Environmental Science and Technology 44(8), 847-907.

Lothenbach, B. and Nonat, A. (2015) Calcium silicate hydrates: Solid and liquid phase composition. Cement and Concrete Research 78, 57-70.

Mahmood, T., Saddique, M.T., Naeem, A., Westerhoff, P., Mustafa, S. and Alum, A. (2011) Comparison of Different Methods for the Point of Zero Charge Determination of NiO. Industrial & Engineering Chemistry Research 50(17), 10017-10023.

Murad, E. (1988) Iron in Soils and Clay Minerals. Stucki, J.W., Goodman, B.A. and Schwertmann, U. (eds), pp. 309-350, Springer Netherlands, Dordrecht.

Murad;, E. and Schwertmann, U. (1980) The Moessbauer spectrum of ferrihydrite and its relations to those of other iron oxides. American Mineralogist 65(9-10), 1044-1049.

Parfitt, R.L., Atkinson, R.J. and Smart, R.S.C. (1975) The Mechanism of Phosphate Fixation by Iron Oxides 1. Soil Science Society of America Journal 39(5), 837-841.

Rietra, R.P.J.J., Hiemstra, T. and van Riemsdijk, W.H. (2001) Interaction between Calcium and Phosphate Adsorption on Goethite. Environmental Science & Technology 35(16), 3369-3374.

Schwertmann, U., Carlson, L. and Fechter, H. (1984) Iron oxide formation in artificial ground waters. Schweizerische Zeitschrift für Hydrologie 46(2), 185-191.

Sengupta, S. and Pandit, A. (2011) Selective removal of phosphorus from wastewater combined with its recovery as a solid-phase fertilizer. Water Research 45(11), 3318-3330.

Shuang, C., Wang, M., Zhou, Q., Zhou, W. and Li, A. (2013) Enhanced adsorption and antifouling performance of anion-exchange resin by the effect of incorporated Fe3O4 for removing humic acid. Water Research 47(16), 6406-6414.

Sigg, L. and Stumm, W. (1981) The interaction of anions and weak acids with the hydrous goethite (α-FeOOH) surface. Colloids and Surfaces 2(2), 101-117.

Tawfik, D.S. and Viola, R.E. (2011) Arsenate Replacing Phosphate: Alternative Life Chemistries and Ion Promiscuity. Biochemistry 50(7), 1128-1134.

Wan, J., Tao, T., Zhang, Y., Liang, X., Zhou, A. and Zhu, C. (2016) Phosphate adsorption on novel hydrogel beads with interpenetrating network (IPN) structure in aqueous solutions: kinetics, isotherms and regeneration. RSC Advances 6(28), 23233-23241.

Wang, X., Liu, F., Tan, W., Li, W., Feng, X. and Sparks, D. (2013) Characteristics of Phosphate Adsorption-Desorption Onto Ferrihydrite: Comparison With Well-Crystalline Fe (Hydr)Oxides. Soil Science 178, 1-11.